Correlation between Metal NMR Physical Quantities and Structures of Metal Complexes. I. ^{109}Ag NMR Spectroscopy of Aqueous Silver Ions Coordinated with Nitroxide Radical

KAZUNAKA ENDO AND KYONOSUKE YAMAMOTO

R & D Laboratories for Photo Materials, Mitsubishi Paper, Ltd., Nagaokakyo, Kyoto 617, Japan

KAZUHIRO MATSUSHITA AND KENZO DEGUCHI

NMR Application Laboratory, Scientific Instrument Division, JEOL Ltd., Akishima, Tokyo 196, Japan

AND

KATSUYA KANDA AND HIROSHI NAKATSUJI

Department of Molecular Engineering, Faculty of Engineering, Kyoto University, Kyoto 606, Japan

Experimental ^{109}Ag NMR and theoretical MO methods have been used to investigate the electronic structure of silver complexes in aqueous solution. ^{109}Ag spectra of ionic silver solutions ($\leqslant 1.0$ M) can be obtained with a short repetition time (2–3 s) when 0.020 M 2,2,6,6-tetramethyl-4-hydroxypiperidine-1-oxyl is added as a doping agent. By consideration of multiple equilibria, ^{109}Ag chemical shifts of silver complexes in aqueous solution were found to cover a range of 0 to 1300 ppm, relative to 1.0 M AgNO$_3$. Tetrahedral silver complexes were at lowest field with linear silver complexes more shielded and hydrated silver ion at highest field. Our study suggests a correlation between ^{109}Ag chemical shielding and the structure of silver complexes in aqueous solution. An ab initio SCF MO method using a STO-3G basis set is used to clarify the nature of the ligand–silver interaction and to interpret the observed ^{109}Ag chemical shifts. The results indicate that electron density transfers from the lone pair of the ligand to vacant 5s and 5p orbitals on silver. Also back donation to ligand produces a hole in the 4d orbitals coincident with the bonding axes of silver complexes. The ^{109}Ag chemical shieldings are found to be explained by the paramagnetic term, which depends upon p electrons and d holes on the Ag atom according to qualitative perturbation theory. © 1985 Academic Press, Inc.

The study of the correlation between metal NMR, physical quantities, and structures of metal complexes in solids and solution is of particular interest from experimental and theoretical points of view (*1*). As a part of our continuing investigation of this problem, we report here an extensive study of NMR and molecular orbital properties showing correlation between ^{109}Ag chemical shifts and electronic structures of silver complexes in aqueous solution.

The silver ion and its complexes are not only important in inorganic chemistry, but play a role in organic chemistry and are important in photographic chemistry.

Yet, good physical probes, e.g., spectroscopic approaches, have not been available for delineating the role of Ag(I) species in chemical processes. For example, Ag(I) does not exhibit convenient properties for uv-visible spectroscopy, and has no EPR spectrum. In nuclear magnetic resonance, both silver nuclei, [107]Ag and [109]Ag, are accessible to NMR investigations, but they have relatively small magnetic moments and very low sensitivity. Another difficulty with [109]Ag NMR measurements arises from the fact (2) that this nucleus has an extremely long relaxation time. In spite of these experimental difficulties, there have been several papers (2–9) on NMR studies of silver nuclei.

The current study presents some representative [109]Ag NMR spectra obtained in 30 min or less from solutions of silver salts (1.0 M) containing the free radical TANOL (2,2,6,6-tetramethyl-4-hydroxypiperidine-1-oxyl) (10). The [109]Ag chemical shifts of these silver complexes were analyzed with consideration of the multiple equilibria in aqueous solution.

To determine the mole fractions of various complexes, we have performed electrode potential (E_{Ag}) measurements and done numerical calculations using the equilibrium constants obtained. The experimental deshielding order was tetrahedral silver complexes > linear silver complexes > hydrated silver ion. Furthermore, the results indicate that the silver ion forms a bimolecular coordinate bond with TANOL. A positive scalar hyperfine coupling constant of 0.86 MHz can be estimated for the [109]Ag nucleus with a lifetime of 1.7×10^{-9} s.

We have carried out ab initio SCF MO calculations for the electronic states of hydrated silver ion and silver complex species to explain the nature of the ligand–silver interaction in aqueous solution. This nature is clarified qualitatively with the use of the orbital energy level diagrams. To give a physical picture for [109]Ag shieldings of silver complexes, a rough calculation was performed by use of perturbation theory (11) with the average excitation energy approximation.

EXPERIMENTAL METHODS

TANOL was prepared according to Neiman *et al.* (10). All other chemicals were commercially available.

Natural abundance [109]Ag spectra were obtained at 4.11 MHz from samples in 10 mm tubes on a JEOL FX 90Q spectrometer in quadrature Fourier transform mode. The measurements were made at ambient temperature, 30°C. 500–700 transients were accumulated with a pulse interval of 2–3 s and pulse angle of 45° (90 μs). All chemical shifts for [109]Ag are defined by the equation $\Delta\sigma_{sam} = (\nu_{sam} - \nu_{ref})/\nu_{ref}$, where ν_{sam} is the resonance frequency of the sample and ν_{ref} is the reference frequency. Shifts defined in this manner increase for lower shielding; 1.0 M AgNO$_3$ is taken as the chemical-shift reference. The chemical-shift correction may not be exact because TANOL may affect a shift of a complex differently than that of solvated Ag$^+$. When samples of 1.0 M silver salt solutions contained 0.020 M of TANOL as a doping agent, we corrected the chemical shifts as 10 ± 1.3 ppm from Fig. 1: $\Delta\sigma \simeq$ (Const.)$\cdot (N/N_0)$, where N, N_0 are the concentrations of TANOL and AgNO$_3$, respectively. The bulk susceptibility corrections were made with ^{1}H water resonance within the error of the experiments (± 0.5 ppm). The T_1 was measured by 180°–τ–90° pulse sequence and T_2 was evaluated from signal width at half-height. The lineshape of the [109]Ag spectra was assumed to be Lorentzian. Solutions for the silver spectra in Table 1 were freshly

made before use by completely dissolving much amount of ligands (more than 2.0 M), then dissolving the silver salts because some silver salts are sparingly soluble in water.

Measurements of pH were performed with a HM-5A (TOA Electronics Ltd.) pH meter. The glass electrode HG-2005 was adjusted with commercial standard solutions. As a reference electrode a sleeve silver electrode HS-205C was used. A homemade solid-state silver electrode was used with a double junction silver chloride reference electrode HS-305DS (TOA Electronics Ltd.). These electrodes were standardized with a solution of a known concentration of silver nitrate in 1.0 M KNO_3. The potential E_{Ag} value was determined as $E_{Ag} = 0.592 + 0.0601(log[Ag^+])$, where $[Ag^+]$ denotes molarity. All measurements were performed in thermostated vessels at $30 \pm 0.1°C$ and at an ionic strength of 1.0 M KNO_3.

RESULTS AND DATA ANALYSIS

Silver–TANOL complex. We investigated the radical effect on [109]Ag resonance positions and relaxation rates in a 1.0 M concentration of silver nitrate. The [109]Ag NMR signal of $AgNO_3$ in aqueous solution showed a high-frequency shift and a broadening with further addition of TANOL. As is shown in Fig. 1, this high-frequency shift is proportional to the concentration of added TANOL. The shift is most likely caused by the Fermi contact interaction (theory of Bloembergen (*12*)) for the silver nucleus which is coordinately bonded to TANOL radical. The [109]Ag chemical shift was 24.5 ppm for $AgNO_3$/TANOL aqueous solution in which the molar ratio of $AgNO_3$ to TANOL is 20. At this concentration of TANOL, the [109]Ag T_1 is 83 ± 0.5 ms and the T_2 is 1.6 ± 0.3 ms. The T_1/T_2 ratio is 52, indicating the predominance of a Fermi contact term in the linewidth according to the Solomon–Bloembergen (S–B) equa-
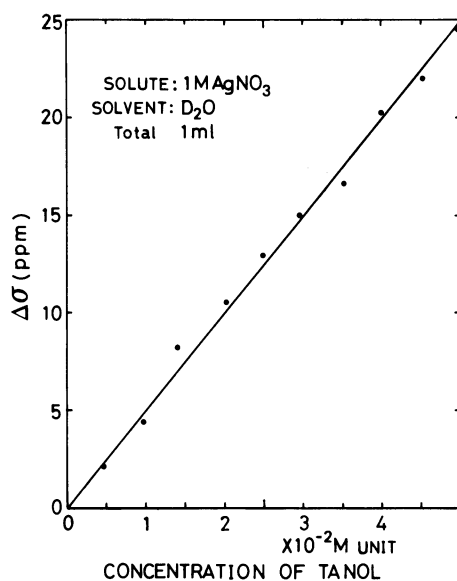

FIG. 1. [109]Ag chemical shift at 30°C versus the concentration of added TANOL radical.

tions (13). These results indicate that the silver ion forms a bimolecular complex with TANOL.

In the case of this bimolecular complex formation (14), the scalar coupling constant for the ^{109}Ag nucleus can be estimated as can the lifetime in the Ag$^+$–TANOL complex. The relation of the shift to the scalar coupling is approximated by Solomon's equation:

$$\Delta H/H = -\frac{\gamma_e A_{Ag} N n}{4\gamma_{Ag} kT\, N_0} \qquad [1]$$

where N and N_0 are the numbers of radical and Ag$^+$ particles/cm^3, respectively; n is the number of Ag$^+$ ions in the solvation sphere (the reasonable value (15) of n is 4–10); γ_{Ag}, γ_e are the magnetogyric ratios of the silver and electron spin. We, thus, obtained a positive scalar hyperfine coupling constant, A_{Ag}, of 0.86 MHz for $n = 4$. The rate of chemical exchange (τ_e) in the Ag$^+$–TANOL complex is estimated with the help of the S–B equations. The equations are given as

$$N_0/NT_1 = (n\gamma_{Ag}^2\gamma_e^2\hbar^2/10r^6)(3J_d(0) + 7J_d(\omega_s)) + (nA_{Ag}^2/2\hbar^2)(J_e(\omega_s)), \qquad [2]$$

$$N_0/NT_2 = (n\gamma_{Ag}^2\gamma_e^2\hbar^2/20r^6)(7J_d(0) + 13J_d(\omega_s)) + (nA_{Ag}^2/4\hbar^2)(J_e(0) + J_e(\omega_s)), \qquad [3]$$

where

$$J_d(\omega_s) = \tau_c/(1 + \omega_s^2\tau_c^2), \qquad [4]$$

$$J_e(\omega_s) = \tau_e/(1 + \omega_s^2\tau_e^2), \qquad [5]$$

where r is the effective separation between the silver nucleus and the odd electron; τ_c is the dipolar correlation time of the silver ion–TANOL complex; $J_d(\omega_s)$, $J_e(\omega_s)$ are the reduced spectral density functions for pure dipolar and scalar coupling for the silver ion–TANOL complex model at electron Lamor frequency; $J_d(0)$, $J_e(0)$ are the spectral density functions for pure dipolar and scalar couplings for the silver ion–TANOL complex model at zero frequency.

Dipolar terms can be assumed to give nearly equal contributions to T_1 and T_2. Considering Eqs. [2] and [3], we obtain

$$(1/T_2)_{\text{obsd}} - (1/T_1)_{\text{obsd}} \simeq (A_{Ag}/2\hbar)^2 \frac{Nn}{N_0}\left(\tau_e - \frac{\tau_e}{1 + \omega_s^2\tau_e^2}\right). \qquad [6]$$

When the value of ω_s, 3.7×10^{11} rad/s at 21.14 kG, is held in Eq. [6], the resulting value of τ_e, 1.7×10^{-9} s, appears to correspond to those for the paramagnetic metal ion–water complexes obtained by NMR experiments (16) ($\tau_e \simeq 10^{-9}$ s). This satisfies the condition $\omega_s^2\tau_e^2 \gg 1$ in this silver–TANOL complex system.

Aqueous silver complexes. Table 1 presents the corrected chemical-shift data for a number of ^{109}Ag resonances in silver salt solutions. The range of ^{109}Ag chemical shifts is around 1300 ppm, including dissociated silver nitrate at 0 ppm. Silver ion in KCN solution gives rise to the most deshielded resonance. These data are consistent with the ^{109}Ag chemical shifts being dominated by local paramagnetic contributions (11) to the shielding constant. An isolated Ag$^+$ ion would have little paramagnetic contribution to its shielding constant (11). Symmetrically hydrating the Ag$^+$ ion will have the effect of introducing a small paramagnetic contribution to the observed shielding constant. Introduction of coordinate bonds will, in turn, gives rise to large and negative

ENDO ET AL.

TABLE 1

[109]Ag Chemical Shifts and Mole Fractions of Silver Complexes
for Various Silver Salts in Aqueous Solution

Solution (in H_2O)		Chemical shift (ppm)	Mole fraction (%)		
Silver salt	Addend		$AgL_2^{(2i-1)-}$	$AgL_3^{(3i-1)-}$	$AgL_4^{(4i-1)-}$
$AgNO_3$ (1.0 M)		0			
$AgNO_3$ (1.0 M)/$N(CH_2CH_2OH)_3$ (4.0 M)		232	99.2		
$AgNO_3$ (1.0 M)/$HN(CH_2CH_2OH)_2$ (4.0 M)		306	99.9		
$AgNO_3$ (1.0 M)/$H_2NCH_2CH_2OH$ (4.0 M)		363	100		
$AgNO_3$ (1.0 M)/NH_3 (16.0 M)		505	100		
$AgNO_3$ (0.50 M)/Na_2SO_3 (satur.)		571	28	72	
AgBr (0.20 M)/NaBr (4.0 M)[a]		623	0.2	7.6	92.1
AgI (1.0 M)/NaI (4.0 M)		739	0.0	8.5	91.5
$AgNO_3$ (1.0 M)/$Na_2S_2O_3$ (4.0 M)		826	17.7	82.3	
$AgNO_3$ (1.0 M)/KSCN (6.0 M)		951	0.0	10.7	89.3
$AgNO_3$ (1.0 M)/KCN (6.0 M)		1224	2.0	12.5	85.4

[a] 27,500 transients of 5s were corrected for [109]Ag spectrum of the aqueous solution of 0.20 M AgBr in 4.0 M NaBr. More positive values refer to lower shielding. A 1.0 M $AgNO_3$ solution is taken as the chemical shift reference for all [109]Ag measurements.

paramagnetic contributions to the shielding constant. The cyanide, thiocyanate, and thiosulfate shieldings are consistent with this view.

It must be kept in mind that the shifts of the systems in Table 1 represent weighted averages of the shifts for the various species in equilibrium in the solution. In aqueous solutions of silver ion and ligands (under the condition of $[L^{i-}] \gg [Ag^+]$), a variety of silver complexes of the form $AgL_m^{(im-1)-}$ are generally considered to exist. When we consider the complex reaction between a silver ion and ligands, the total silver ion concentration, $[Ag^+]_0$, in a solution is given by:

$$[Ag^+]_0 = [Ag^+](1 + \sum_{n=1}^{N} \beta_n[L^{i-}]^n) \qquad [7]$$

where $[Ag^+]$ is the free silver ion concentration, $[L^{i-}]$ is the free ligand concentration, N is the number of complex species, and β_n is the nth formation constant.

We have measured the E_{Ag} value as a function of the free ligand concentration, to obtain the formation constants of silver complex in solution. We can determine the formation constants from Eq. [7] with varying initial concentrations ($[Ag^+]_0$, $[L^{i-}]$) for aqueous solutions of silver ion and ligands (under the concentration where $[L^{i-}] \gg [Ag^+]_0$). The formation constants that were determined in this way are reported in Table 2 and are in good accordance with the values in Ref. (17). By use of these equilibrium constants, we have calculated the distribution of silver complexes in each NMR sample. The results were shown in Table 1. [109]Ag Chemical shifts of the predominant species of silver complexes are also plotted in Fig. 2.

In Fig. 2, the observed deshielding order is: tetrahedral silver complexes > linear silver complexes > hydrated silver ion. This feature suggests correlation between [109]Ag chemical shifts and structures of silver complexes in aqueous solution. Furthermore,

TABLE 2

Formation Constants of Silver Complexes in Aqueous Solution at 30°C

Ligand	$\log \beta_1$	$\log \beta_2$	$\log \beta_3$	$\log \beta_4$
$N(CH_2CH_2OH)_3{}^a$	2.45	4.03		
$HN(CH_2CH_2OH)_2{}^a$	2.83	5.41		
$H_2NCH_2CH_2OH{}^a$	3.02	7.03		
$NH_3{}^a$	3.25	7.40		
$SO_3{}^{2-}$	5.41	8.43	8.82	
Br^-	4.54	7.60	8.41	8.86
I^-	7.13	11.85	14.11	14.93
$S_2O_3{}^{2-}$	8.04	12.75	13.90	
SCN^-	5.50	9.06	10.35	11.06
CN^-	8.82	19.05	20.30	20.80

^{a} Denotes the formation constants corrected by means of pH measurements. (The error of this experiment is ±0.005.)

it is pointed out that the shielding order $(Ag(TEA)_2{}^+ > Ag(DEA)_2{}^+ > Ag(EA)_2{}^+ > Ag(NH_3)_2{}^+ > AgBr_4{}^{3-} > AgI_4{}^{3-} > Ag(SCN)_4{}^{3-} > Ag(CN)_4{}^{3-})$ corresponds well to the order of increasing stability to silver ion with ligands (TEA < DEA < EA < NH_3 < Br^- < SCN^- < I^- < CN^- except for the characteristic shielding order of $AgI_4{}^{3-}$ > $Ag(SCN)_4{}^{3-}$).

Electronic state and ligand–silver interaction for silver complex species by ab initio SCF MO calculations. To explore the electronic structure of silver complexes in aqueous solution, we have carried out Hartree–Fock SCF MO calculations for the electronic states of hydrated silver ion and silver complex species using a slightly modified version of the HONDO program (*18*). The basis set is at the minimal STO-3G level (*19*). We assume that geometries of hydrated silver ion, silver diammonia and dichloride, and silver tetrachloride are octahedral, linear, and tetrahedral, respectively. These geometries are based on experimental data for metal complex species in
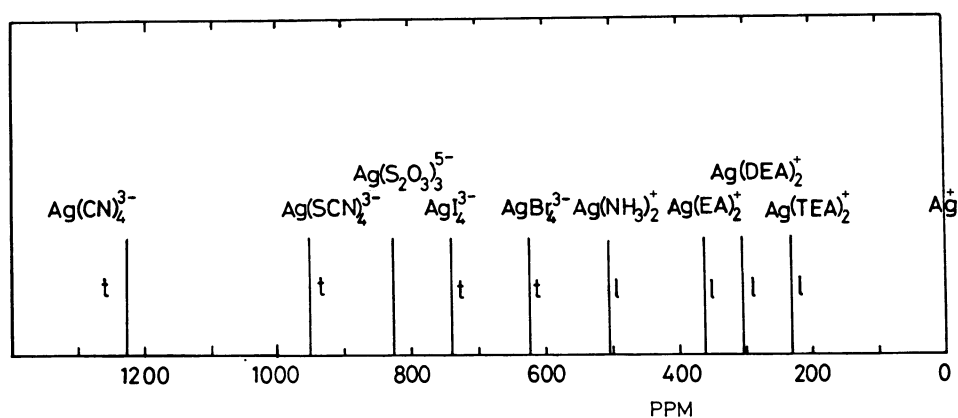

FIG. 2. ^{109}Ag chemical shifts of predominant species of silver complexes in aqueous solution relative to that of 1.0 M AgNO$_3$. ("l" and "t" mean linear and tetrahedral silver complexes, respectively).

TABLE 3

Assumed Structures and Bond Lengths
of Silver Complexes

Silver complex	Structure	Bond length (Å)
$Ag(H_2O)_6^+$	Octahedral (O_h)	r(Ag—O) 2.36
$Ag(NH_3)_2^+$	Linear (D_{3d})	r(Ag—N) 2.22
$AgCl_2^-$	Linear ($D_{\infty h}$)	r(Ag—Cl) 2.28
$AgCl_4^{3-}$	Tetrahedral (T_d)	r(Ag—Cl) 2.28
$Ag(CN)_4^{3-}$	Tetrahedral (T_d)	r(Ag—C) 2.29

solution (20–22). Bond distances used here are shown in Table 3. These values are cited from Pauling's textbook (23).

Table 4 summarizes the change in valence atomic orbital population of silver ion and ligands due to hydration and ligand addition. In Table 4 the population increases in $5s$ and $5p$ AOs of silver atoms and population decreases in the s and p AOs of ligands indicate electron transfer from ligand to silver. There is no change in the d orbital populations for the hydrated silver ion, while the population in the $4d$ orbitals of the bonding axes of the silver complexes decreases (Table 4). This means that a hole is produced in the d bonding orbitals.

We also aim to clarify the nature of the ligand–silver interaction with the use of orbital energy level diagram. Figures 3–5 show typical examples of ligand–silver interaction. Here the orbital energies of the ligand were estimated from the electron affinity and ionization potentials.

TABLE 4

The Change in AO Populations[a] of Silver Complexes

Orbital	$Ag(H_2O)_6^+$	$Ag(NH_3)_2^+$	$AgCl_2^-$	$AgCl_4^{3-}$	$Ag(CN)_4^{3-}$
Ag					
$4d_{xx+yy}$	0.000	0.000	0.000	0.000	0.000
$4d_{zz}$	0.000	−0.166	−0.158	0.000	0.000
$4d_{xy}$	0.000	0.000	0.000	−0.053	−0.060
$4d_{xz}$	0.000	0.000	0.000	−0.053	−0.060
$4d_{yz}$	0.000	0.000	0.000	−0.053	−0.060
$5s$	0.177	0.304	0.528	0.177	0.218
$5p_x$	0.120	0.031	0.120	0.246	0.262
$5p_y$	0.120	0.031	0.120	0.246	0.262
$5p_z$	0.120	0.098	0.169	0.246	0.262
Ligand	(O--n = 2)	(N--n = 2)	(Cl--n = 3)	(Cl--n = 3)	(C--n = 2)
ns	−0.107	−0.160	−0.033	−0.016	−0.427
np_x	−0.425	−0.735	−0.028	−0.106	−1.138
np_y	−0.716	−0.735	−0.028	−0.106	−1.138
np_z	−0.018	−0.437	−0.200	−0.106	−1.138

[a] In our MO calculation the AO populations of unsolvated ion are given as follows: AO populations of $5s$, $5p_x$, $5p_y$, and $5p_z$ are 0.000 and others are 2.000, respectively.
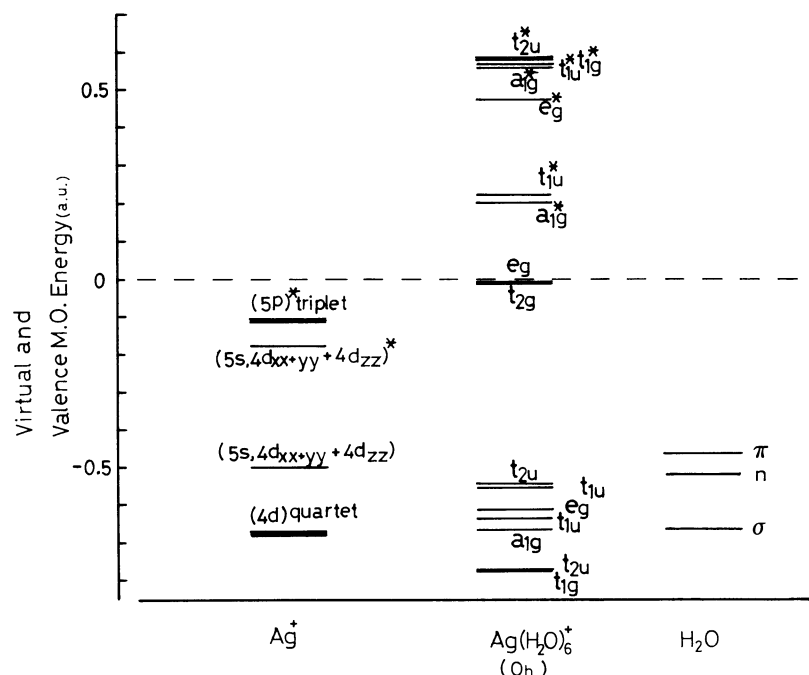
FIG. 3. Orbital energy level diagram for virtual and valence MOs of Ag^+, $Ag(H_2O)_6^+$, and H_2O. * means the virtual MO.

Inspection of Figs. 3–5 indicates the mechanism for the electron transfer and back donation in the formation of ligand–silver complexes. The electron donation occurs from a π orbital or nonbonding n orbital of the ligand to the vacant $(5p)^*$ MO of Ag^+ in a π-like symmetry. In a σ-like symmetry, the electron of the ligand transfers from the σ orbital to the vacant $(5s, 4d_{xx+yy} + 4d_{zz})^*$ MO of silver ion. Furthermore, back donation in the d orbitals of silver to the ligand might promote electron density to the unoccupied π^* and σ^* orbitals of ligand (these unoccupied orbital energy levels have not been shown in Figs. 3–5) from the occupied $(4d)$ and $(5s, 4d_{xx+yy} + 4d_{zz})$ MOs of Ag^+ in π- and σ-like symmetries, respectively. This is the so-called HOMO–LUMO interaction. In the H_2O–silver interaction system (Fig. 3), the energy difference between the LUMOs Ag^+ and HOMOs $(\pi^1$ and $n)$ of H_2O is about 0.3 ∼ 0.4 a.u. In addition, the energy of the σ orbital for H_2O is 0.5 a.u. lower than that of the LUMO for Ag^+. Thus, electron transfer between H_2O and Ag^+ is smaller than in other ligand–Ag^+ interaction systems and back donation to H_2O may be difficult to achieve. In the case of the Ag^+–Cl^- interaction (Fig. 4), the energy level of the LUMO for Ag^+ approaches to that of the HOMO (π^1) for Cl^-. In the formation of $AgCl_2^-$ and $AgCl_4^{3-}$, both electron transfer and back donation may be easily accomplished. For the $Ag(NH_3)_2^+$ complex (Fig. 5), we can regard possibilities for electron transfer (donation)

[1] Here we adopted the π orbitals for the H_2O molecule and Cl^- ion instead of p orbitals of them from a standpoint of the silver–ligand interaction system.

Virtual and Valence M.O.Energy (a.u.)
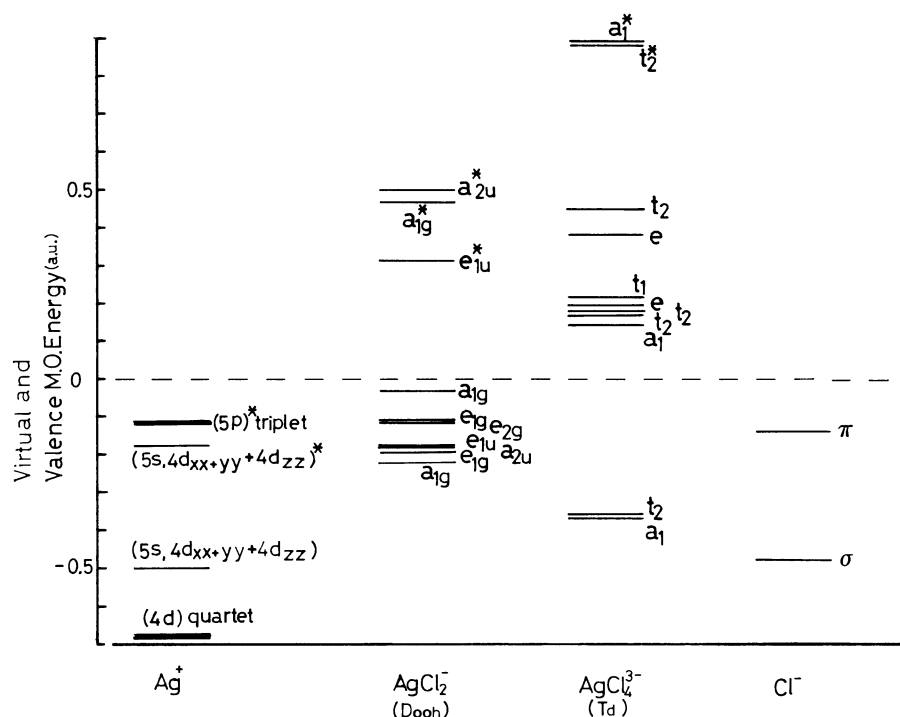
0.5

0

-0.5

a₁*
t₂*

a₂u*
a₁g*
e₁u*

t₂
e

t₁
e
t₂ t₂
a₁

(5p)* triplet
(5s,4d_xx+yy+4d_zz)*

a₁g
e₁g e₂g
e₁u a₂u
e₁g
a₁g

π

(5s,4d_xx+yy+4d_zz)

t₂
a₁

σ

-0.5

(4d) quartet

Ag⁺   AgCl₂⁻   AgCl₄³⁻   Cl⁻
             (D∞h)   (Td)

FIG. 4. Orbital energy level diagram for virtual and valence MOs of Ag^+, $AgCl_2^-$, $AgCl_4^{3-}$, and Cl^-. * means the virtual MO.

and back donation as intermediate between the H_2O-Ag^+ and Cl^--Ag^+ interaction systems. This can be seen in Table 4.

DISCUSSION

It is generally difficult to obtain information about the structure and dynamic behavior of diamagnetic silver complexes in aqueous solution because appropriate physical probes have not been available for delineating the role of the Ag(I) species. However, we wish to stress that with the use of a stable free radical as a NMR doping agent [109]Ag NMR measurements, combined with MO calculations of the electronic states of hydrated Ag^+ and silver complex species, offers a powerful means of studying silver complexes in aqueous solution. In the preceding section, we noted the correlation between chemical shifts and structures of silver complexes from experimental analysis. The ab initio MO calculations afford not only information about the electronic structure of silver complexes, but also probe the nature of the ligand–silver bond in aqueous solution. Here we will give the physical picture for [109]Ag chemical shieldings of silver complexes, from a rough calculation using perturbation theory (*11*).

Silver–TANOL complex in aqueous solution. An analysis of [109]Ag resonance position and relaxation data in $AgNO_3$/TANOL aqueous solution showed that the silver ion forms a bimolecular complex with TANOL. The rate of chemical exchange in the

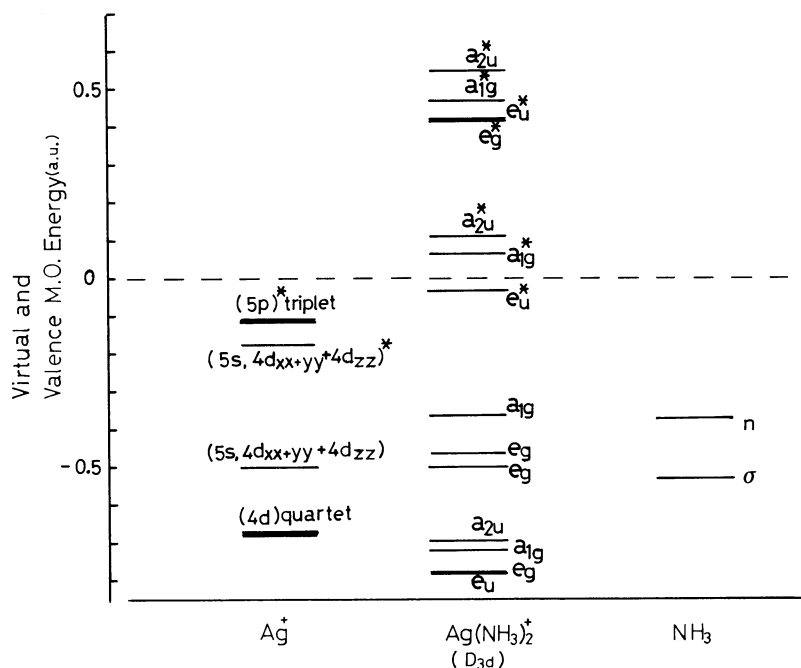FIG. 5. Orbital energy level diagram for virtual and valence MOs of Ag^+, $Ag(NH_3)_2^+$, and NH_3. * means the virtual MO.

Ag^+-TANOL complex was evaluated as $\tau_e \simeq 1.7 \times 10^{-9}$ s. Using Eq. [8], the TANOL-induced positive spin density ρ_{Ag} on the silver nucleus is obtained as 4.3×10^{-4} from the scalar hyperfine coupling constant, A_{Ag}, of 0.86 MHz:

$$A_{Ag} = (8\pi/3)g\beta\gamma_{Ag}|\psi_{Ag}(0)|^2\rho_{Ag}. \tag{8}$$

The notations have their usual meaning (24).

To discuss the structure of the Ag^+-TANOL complex, we can refer to the investigation by Morishima et al. (25) of the hydrogen bond between proton–donor (X–H) and di-tert-butyl nitroxide (DTBN) radical molecules. The analogy is based upon the fact that the s orbital for each atom dominates the bonding in respective chemical interactions. If we consider the silver ion instead of the proton of XH, we can fit the SCF MO calculations (25) which have been performed for the dimethyl nitroxide (DMNO)–XH bimolecular system to the Ag^+-TANOL complex system. Thus, the positive spin density (on the silver nucleus) which was confirmed by our [109]Ag de-shielding shift may be reproduced for the σ model where the silver ion is placed on the σ plane and directed toward an oxygen lone-pair orbital in Fig. 6 (the N–O---Ag^+ angle = 120°). In the XH/DMNO system, the σ model was more stable than the π model (where the XH proton is directly over the p–π orbital of the oxygen atom) by MO calculation of stabilization energy for the σ and π models. Thus, the model in Fig. 6 may be responsible for the observed positive spin density on the silver nucleus.
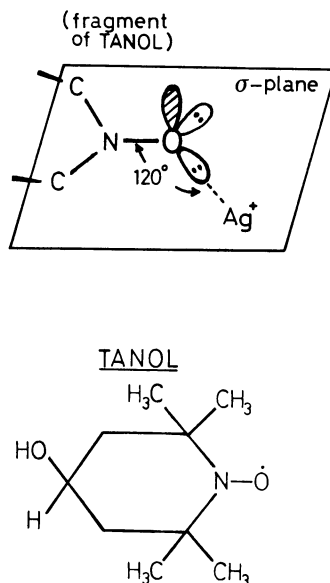
FIG. 6. σ model for the structure of the Ag^+–TANOL complex system.

Simplified interpretation for ^{109}Ag *chemical shieldings of silver complexes in aqueous solution.* According to Ramsey's definition (26) the diamagnetic part of the shielding constant involves only the unperturbed ground state, while the temperature-independent paramagnetic part contains the perturbed molecular coefficients which depend on the excited states of the molecule. The latter term involves the mixing of ground and excited states by the applied magnetic field. The valence electrons of transition metal atoms occupy p, d, and f orbitals with nonzero intrinsic angular momenta, giving rise to large deviations from spherical symmetry. Therefore, transition metal chemical shifts are most often dominated by second-order paramagnetic contributions. Within the frameworks of LCAO and MO theories, an approximate method has been extended by Jameson and Gutowsky (11) to include d as well as p orbital influence. We also obtained such expression of the paramagnetic term for the Gaussian orbital functions:

$$\sigma_{\text{para}} \simeq -\frac{2\alpha^2}{3}\left(\frac{\langle 1/r^3\rangle_p}{E_p}\cdot P_{\text{u}} + \frac{\langle 1/r^3\rangle_d}{E_d}\cdot D_{\text{u}}\right). \tag{9}$$

Here E_p and E_d are assumed to be the dominant excitation energies of valence p and d electrons, respectively. Other notations correspond to Ref. (11).

To give a physical picture for the metal chemical shieldings of metal complexes, we need to understand the correlation between σ_{para} and populations of p electrons and d holes on metal atoms. Then, we set up the following assumptions in Eq. [9]:

1. The populations of the d electrons in D_{u} (unbalance of electron distribution) are replaced by populations of the d holes. For example, $(2 - p^h_{zz,zz})$ instead of $p_{zz,zz}$ where $p^h_{zz,zz}$, $p_{zz,zz}$ denote populations of d holes and d electrons, respectively.

2. To a first approximation, we consider the first-order diagonal populations (or densities) in P_u and D_u and neglect the off-diagonal and second-order diagonal terms because they are small contributions. Thus, the expression for the paramagnetic shift is given as

$$\sigma_{\text{para}} \simeq - \frac{2\alpha^2}{3} \left(\frac{\langle 1/r^3 \rangle_p}{E_p} \cdot P_T^e + \frac{\langle 1/r^3 \rangle_d}{E_d} \cdot 3D_T^h \right), \qquad [10]$$

where P_T^e and D_T^h mean the total populations of p electrons and d holes, respectively.

As reported earlier for theoretical metal (Ib and IIb) chemical shieldings by Nakatsuji *et al.* (*1*), the chemical shifts of metal complexes for the ligand–metal interaction system can be governed by the paramagnetic term. For Ag(I) chemical shieldings, the p- and d-orbital contributions are competitive, so the chemical shift is due to the sum of the p and d effects of the ligands. This will also be explained in terms of Eq. [10] for Ag chemical shieldings. The paramagnetic term for ^{109}Ag shieldings can be estimated from $E_{p,d}$ and $\langle 1/r^3 \rangle_{5p,4d}$ as parameters in the equation. We assume that $E_p = E_d = E$, $\langle 1/r^3 \rangle_{5p} \simeq 1.38$ a.u. and $\langle 1/r^3 \rangle_{4d} \simeq 3.67$ a.u. (The latter two terms are obtained from the SCF functions by Clementi *et al.* (*27*).) The results in Table 5 agree qualitatively with the observed values. It is thus suggested that the ^{109}Ag chemical shieldings are interpreted dominantly by the paramagnetic term, which depends upon the $5p$ electrons and $4d$ holes on silver atoms. This tendency corresponds well to the theoretical result using an ab initio finite perturbation SCF method (*1*).

Halogen–silver interaction for silver halide complexes. To see the nature of the halogen–silver interaction for these complexes, the orbital energy level diagram for Ag$^+$ and X$^-$ are shown in Fig. 7. In the figure, the energy levels of π and σ orbitals for halogen ions become higher as X$^-$ changes from Cl$^-$ to I$^-$. Then, we can predict that the populations of $5p$ electrons and $4d$ holes on silver atom will increase, as the silver halide changes from AgCl$_4{}^{3-}$ to AgI$_4{}^{3-}$. The halogen–silver interaction and deshielding order are, thus, given as AgI$_4{}^{3-}$ > AgBr$_4{}^{3-}$ > AgCl$_4{}^{3-}$. The shielding order is in good agreement with that of observed ^{109}Ag chemical shieldings.

TABLE 5

Calculated ^{109}Ag Chemical Shielding Constants of Silver Complexes

	Ag(H$_2$O)$_6{}^+$	Ag(NH$_3$)$_2{}^+$	AgCl$_2{}^-$	AgCl$_4{}^{3-}$	Ag(CN)$_4{}^{3-}$
d contribution ($(2\alpha^2/3E_d)$ unit)	0	−1.83	−1.94	−1.75	−1.98
p contribution ($(2\alpha^2/3E_p)$ unit)	−0.50	−0.22	−0.56	−1.03	−1.09
Paramagnetic ($(2\alpha^2/3E)$ unit)	−0.50	−2.05	−2.60	−2.78	−3.05
$\Delta\sigma$ ($(2\alpha^2/3E)$ unit)	0	−1.55	−2.10	−2.28	−2.45
($(E = 3\ ev)$ ppm)	(0)	(−503)	(−681)	(−739)	(−794)
$\Delta\sigma_{(\text{exptl})}{}^a$ (ppm)	0	−505			−1224

a In this table more negative values refer to lower shielding.
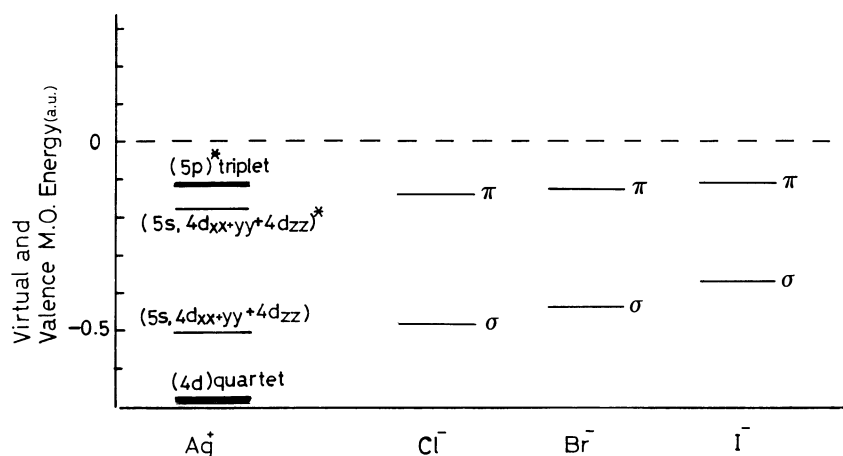
FIG. 7. Orbital energy level diagram for virtual and valence MOs of Ag^+ and $X^-(Cl^-$, Br^-, and I^-). * means the virtual MO.

The results investigated here show that with the use of a stable free radical as a ^{109}Ag NMR doping agent, and with ab initio MO calculations to elucidate the electronic states of silver complexes we can delineate the nature of silver–ligand interactions and interpret Ag chemical shieldings of silver complexes in aqueous solution. Further studies on the metal NMR physical quantities and electronic structures of metal complexes in solid-state and solution are now under way.

ACKNOWLEDGMENTS

REFERENCES

1. H. NAKATSUJI, K. KANDA, K. ENDO, AND T. YONEZAWA, J. Am. Chem. Soc. 106, 4653 (1984).
2. A. K. RAHIMI AND A. I. POPOV, J. Magn. Reson. 36, 351 (1977).
3. C. W. BURGES, R. KOSCHMIEDER, W. SAHM, AND A. SCHWENK, Z. Naturforsch. A 28, 1753 (1973).
4. K. JACKER, W. SAHM, AND A. SCHWENK, Z. Naturforsch. A 31, 1532 (1976).
5. E. BRUM, J. OESER, H. H. STAUB, AND C. G. JELSCHOW, Phys. Rev. 93, 172 (1954).
6. P. B. SOGO AND C. D. JEFFRIES, Phys. Rev. 93, 174 (1954).
7. P. M. HENRICHS, J. J. H. ACKERMAN, AND G. E. MACIEL, J. Am. Chem. Soc. 99, 2544 (1977).
8. P. M. HENRICHS, S. SHEARD, J. J. H. ACKERMAN, AND G. E. MACIEL, J. Am. Chem. Soc. 101, 3222 (1979).
9. K. ENDO, K. MATSUSHITA, K. DEGUCHI, K. YAMAMOTO, S. SUZUKI, AND K. FUTAKI, Chem. Lett., 1497 (1982).
10. M. R. NEIMAN, YU. G. MADEDOVA, AND E. G. ROZANTZEV, Azerb. Khim. Zh., 37 (1962).
11. C. J. JAMESON AND H. S. GUTOWSKY, J. Chem. Phys. 40, 1714 (1964).
12. N. BLOEMBERGEN, J. Chem. Phys. 27, 595 (1957).
13. I. SOLOMON AND N. BLOEMBERGEN, J. Chem. Phys. 25, 261 (1956): I. SOLOMON, Phys. Rev. 99, 261 (1956).

14. K. ENDO, I. MORISHIMA, AND T. YONEZAWA, *J. Chem. Phys.* **67**, 4760 (1977).
15. H. S. GUTOWSKY AND J. C. TAI, *J. Chem. Phys.* **39**, 208 (1963).
16. R. A. BERNHEIM, T. H. BROWN, H. S. GUTOWSKY, AND D. E. WOESSNER, *J. Chem. Phys.* **30**, 950 (1959).
17. L. G. SILLEN AND H. E. MARTELL, Chem. Soc. Spec. Publ. No. 25, 1970.
18. M. DUPUIS, J. RYS, AND H. F. KING, Program No. 336, Quantum Chemistry Program Exchange, University of Indiana, Bloomington, Indiana, 1977.
19. W. J. HEHRE, R. F. STEWART, AND J. A. POPLE, *J. Chem. Phys.* **51**, 2675 (1969); R. F. STEWART, *J. Chem. Phys.* **52**, 431 (1970).
20. D. F. C. MORRIS, E. L. SHORT, AND D. N. WATERS, *J. Inorg. Nucl. Chem.* **25**, 975 (1963).
21. J. J. H. ACKERMAN, T. V. ORR, V. J. BARTSUKA, AND G. E. MACIEL, *J. Am. Chem. Soc.* **101**, 341 (1979).
22. H. MONTGOMERY AND F. C. LINGAFELTER, *Acta Crystallogr.* **20**, 728 (1966).
23. L. PAULING, "The Nature of the Chemical Bond," 3rd ed. Cornell Univ. Press, Ithaca, N.Y., 1960.
24. H. M. McCONNEL AND D. B. CHESTNUT, *J. Chem. Phys.* **28**, 107 (1958).
25. I. MORISHIMA, K. ENDO, AND T. YONEZAWA, *J. Chem. Phys.* **58**, 3146 (1973); *J. Am. Chem. Soc.* **93**, 2048 (1971); *Chem. Phys. Lett.* **9**, 143, 203 (1971).
26. N. F. RAMSEY, *Phys. Rev.* **78**, 689 (1950).
27. E. CLEMENTI, D. L. RAIMONDI, AND W. P. REINHARDT, *J. Chem. Phys.* **47**, 1300 (1967).